

Acoustic Attenuation by Two-dimensional Arrays of Rigid Cylinders

You-Yu Chen and Zhen Ye

Wave Phenomena Laboratory, Department of Physics, National Central University, Chungli, Taiwan 32054
(January 30, 2001)

In this Letter, we present a theoretical analysis of the acoustic transmission through two-dimensional arrays of straight rigid cylinders placed parallelly in the air. Both periodic and completely random arrangements of the cylinders are considered. The results for the sound attenuation through the periodic arrays are shown to be in a remarkable agreement with the reported experimental data. As the arrangement of the cylinders is randomized, the transmission is significantly reduced for a wider range of frequencies. For the periodic arrays, the acoustic band structures are computed by the plane-wave expansion method and are also shown to agree with previous results.

43.20.+g, 42.25.Bs, 52.35.Dm

When propagating through media containing many scatterers, waves will be scattered by each scatterer. The scattered waves will be scattered again by other scatterers. This process is repeated to establish an infinite recursive pattern of rescattering between scatterers, forming a multiple scattering process [1,2]. Multiple scattering of waves is responsible for a wide range of fascinating phenomena, including twinkling light in the evening sky, modulation of ocean ambient sound [3], acoustic scintillation from fish schools [4]. On smaller scales, phenomena such as white paint, random laser [5], electron transport in impured solids [6] are also results of multiple scattering. When waves propagate through media with periodic structures, the multiple scattering leads to the ubiquitous phenomenon of band structures. That is, waves can propagate in certain frequency ranges and follow a dispersion relation, while within other frequency regimes wave propagation is stopped. The former ranges are called allowed bands and the latter the forbidden bands. In certain situations, the inhibition of wave propagation occurs for all directions, leading to the phenomenon of complete band gaps.

The wave dispersion bands are first studied for electronic waves in solids, providing the basis for understanding the properties of conductors, semi-conductors, and insulators [7]. In late 1980s, it became known that such a wave band phenomenon is also possible for electromagnetic waves in media with periodically modulated refractive-indices [8]. Since then, optical wave bands have been extensively studied, yielding a rich body of literature. The theoretical calculations have proven to match well with the experimental observations [9].

In contrast, research on acoustic wave band structures has just started. Although theoretical computations of band structures have been documented for periodic acoustic structures [10], the experimental work was only recent, and to date only a limited number of measurements has been reported. One of the first observations was made on acoustic attenuation by a sculpture [11]. The authors obtained a sound attenuation spec-

trum, which was later verified by the band structure computation [12]. Recently, acoustic band structures have been further measured for acoustic transmission through two-dimensional (2D) periodic arrays of rigid cylinders placed in the air [13]. The authors demonstrated the properties of sound attenuation along two high-symmetry directions of the Brillouin zone of the arrays. They also observed a peculiar effect of deaf bands; within the bands, in spite of non-zero band states, wave propagation is prohibited due to particular symmetry of the states [13].

The main purpose of this Letter is to provide a theoretical investigation of sound transmission by 2D arrays of rigid cylinders in air in line with the experiment of [13], thus providing a direct comparison of attenuation between theory and experiment. Such a direct comparison is relatively scarce in the literature. We note that the comparison between the attenuation spectrum and the dispersion bands is of indirect nature, as the two are not necessarily one to one correspondent, as seen, for instance, when some seemingly allowed bands are actually deaf to wave transmission [13]. This will be further clarified in the later results. Another goal is to study how the randomness affects the acoustic transmission, so to gain some insight into the connection between the forbidden bands and wave localization in 2D [14]. For the purposes, we adopt a self-consistent multiple scattering theory [15].

Consider N straight cylinders located at \vec{r}_i with $i = 1, 2, \dots, N$ to form either a regular lattice or a random array perpendicular to the $x - y$ plane; the regular arrangement can be adjusted to comply with the experiment [13]. The cylinders are along the z -axis. An acoustic source transmitting monochromatic waves is placed at \vec{r}_s , some distance from the array. The scattered wave from each cylinder is a response to the total incident wave composed of the direct wave from the source and the multiply scattered waves from other cylinders. The final wave reaches a receiver located at \vec{r}_r is the sum of the direct wave from the source and the scattered waves from all the cylinders. Such a scattering problem can be formulated *exactly* in the cylindrical coordinates, fol-

lowing Twersky [15]. While the details are in [16], the essential procedure is presented below.

The scattered wave from the j -th cylinder ($j = 1, 2, \dots, N$) can be written as

$$p_s(\vec{r}, \vec{r}_j) = \sum_{n=-\infty}^{\infty} i\pi A_n^j H_n^{(1)}(k|\vec{r} - \vec{r}_j|) e^{in\phi_{\vec{r}-\vec{r}_j}}, \quad (1)$$

where $i = \sqrt{-1}$, $H_n^{(1)}$ is the n -th order Hankel function of the first kind, $\phi_{\vec{r}-\vec{r}_j}$ is the azimuthal angle of the vector $\vec{r} - \vec{r}_j$ relative to the positive x -axis. The total incident wave around the i -th cylinder ($i = 1, 2, \dots, N; i \neq j$) is

$$p_{in}^i(\vec{r}) = p_0(\vec{r}) + \sum_{j=1, j \neq i}^N p_s(\vec{r}, \vec{r}_j), \quad (2)$$

which can be expressed again in terms of a modal series

$$p_{in}^i(\vec{r}) = \sum_{n=-\infty}^{\infty} B_n^i J_n(k|\vec{r} - \vec{r}_i|) e^{in\phi_{\vec{r}-\vec{r}_i}}. \quad (3)$$

The expansion is in terms of Bessel functions of the first kind J_n to ensure that $p_{in}^i(\vec{r})$ does not blow up as $\vec{r} \rightarrow \vec{r}_i$.

To solve for A_n^i and B_n^i , we express the scattered wave $p_s(\vec{r}, \vec{r}_j)$, for each $j \neq i$, in terms of the modes with respect to the i -th scatterer by the addition theorem for the Bessel functions [17]. The resulting formula for the scattered wave $p_s(\vec{r}, \vec{r}_j)$ is

$$p_s(\vec{r}, \vec{r}_j) = \sum_{n=-\infty}^{\infty} C_n^{j,i} J_n(k|\vec{r} - \vec{r}_i|) e^{in\phi_{\vec{r}-\vec{r}_i}}, \quad (4)$$

with

$$C_n^{j,i} = \sum_{l=-\infty}^{\infty} i\pi A_l^j H_{l-n}^{(1)}(k|\vec{r}_i - \vec{r}_j|) e^{i(l-n)\phi_{\vec{r}_i-\vec{r}_j}}. \quad (5)$$

The direct incident wave around the location of the i -th cylinder can be expressed in the Bessel function expansion with respect to the coordinates centered at \vec{r}_i

$$p_0(\vec{r}) = \sum_{l=-\infty}^{\infty} S_l^i J_l(k|\vec{r} - \vec{r}_i|) e^{il\phi_{\vec{r}-\vec{r}_i}}, \quad (6)$$

with the known coefficients

$$S_l^i = i\pi H_{-l}^{(1)}(k|\vec{r}_i - \vec{r}_s|) e^{-il\phi_{\vec{r}_i-\vec{r}_s}}.$$

Matching the coefficients in equation (2), using equations (3), (4) and (6), we have

$$B_n^i = S_n^i + \sum_{j=1, j \neq i}^N C_n^{j,i}. \quad (7)$$

At this stage, both the S_n^i are known, but both B_n^i and A_n^j are unknown. Boundary conditions will give another

equation relating them. The boundary conditions state that the pressure and the normal velocity be continuous across the interface between a scatterer and the surrounding medium. After a deduction, we obtain

$$B_n^i = i\pi \Gamma_n^i A_n^i, \quad (8)$$

where

$$\Gamma_n^i = \frac{H_n^{(1)}(ka^i)J_n'(ka^i/h^i) - g^i h^i H_n^{(1)'}(ka^i)J_n(ka^i/h^i)}{g^i h^i J_n'(ka^i)J_n(ka^i/h^i) - J_n(ka^i)J_n'(ka^i/h^i)}. \quad (9)$$

Here the primes refer to taking derivative, a^i is the radius of the i -th cylinder, $g^i = \rho_1^i/\rho$ is the density ratio, and $h^i = k/k_1^i = c_1^i/c$ is the sound speed ratio for the i -th cylinder.

The unknown coefficients A_n^i and B_n^j can be inverted from Eqs. (5), (7), and (8). Once A_n^i are determined, the transmitted wave at any spatial point is given by

$$p(\vec{r}) = p_0(\vec{r}) + \sum_{i=1}^N \sum_{n=-\infty}^{\infty} i\pi A_n^i H_n^{(1)}(k|\vec{r} - \vec{r}_i|) e^{in\phi_{\vec{r}-\vec{r}_i}}. \quad (10)$$

The acoustic intensity is represented by the squared module of the transmitted wave. When the cylinders are placed regularly, we can also obtain the band structures by the plane wave method well documented in [10]. The programs used are identical to that used for computing the acoustic bands in the regular arrays of air-cylinders in water [18]

Numerical computation has been carried out for the experimental situations [13] and also for an random array of the cylinders. In the simulation, all the cylinders are assumed to be the same, in accordance with the experiment. Moreover, the radii of the cylinders and the lattice constants are also taken from the experiment. Several values for the acoustic contrasts between the cylinder and the air were used in the initial stage of computation. We found that the results are in fact insensitive to this factor as long as the contrasts exceed a certain value. This agrees with the experimental observation. In the results shown below, we use $g = h = 20$ as the values for the acoustic contrasts. In the computation, we allow the number of the total cylinders to vary from 100 to 500, in line with the experiment. In the particular results shown later, we assume that the cylinders are placed within a rectangular area of 8×40 of lattice domain. The source and receiver are placed about one lattice constant away from the long side of the array so to minimize the effect due to the finite sample size. As we do not know the specifications for the transmitter and the receiver, we assume an omni-directional transmitter as the acoustic source located on one side of the array of the cylinders, whereas

an omni-directional receiver is placed on the other side to receive the propagated waves.

In Fig. 1, we show the relative attenuation ($\sim -\ln |p|^2$) spectra for various square lattices for acoustic transmission along the $[100]$ direction. The parameters for the four cases considered are adopted from the experiment [13]. We observe a robust attenuation peak located around 1.5 kHz for all the situation. By eye inspection of Fig. 1 and Fig 1 in [13], the agreement between the theoretical and the measured results are good, particularly in view of the finite dimension of the arrays and no adjustable parameters. The height of the attenuation peaks depend on the locations of either the receiver and the transmitter, on the outer boundary of the cylinder arrays, and on the number of cylinders. Nevertheless, the theoretical results describe quantitatively well the observation. A slight difference appears, however, for the case with cylinders of diameter 1 cm at the filling of 0.006. In our results, a small attenuation peak occurs at about 1.5 kHz, but is absent from the experiment. This discrepancy may be attributed to a couple of reasons: the theoretical setting does not match exactly that in the experiment and perhaps the attenuation peak is too small to be observable. In Fig. 1 we also observe some peaks located at higher frequencies as observed in the experiment. These peaks are sensitive to the arrangement of the transmitter and receiver, and the number of the cylinders. They are not because the frequencies are within a stop band.

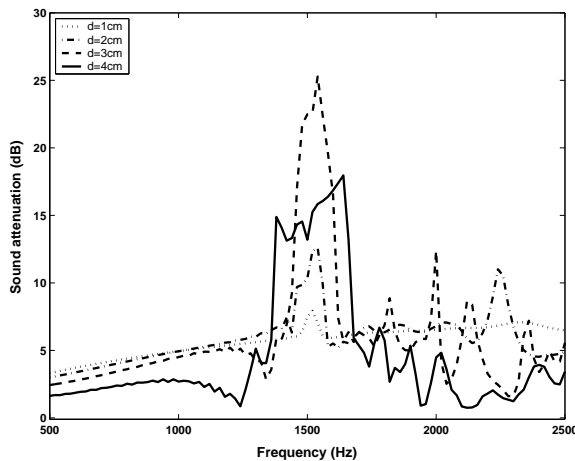


FIG. 1. Theoretical results for the relative acoustic attenuation along $[100]$ as a function of frequency for various arrangements of cylinders. The parameters for the cylinder arrays are taken from the experiment.

Fig. 2 shows the attenuation (relative) spectra for the case of cylinders of diameter 3 cm in a square lattice with lattice constant 11 cm. The corresponding band structure is also depicted. The attenuation along the $[100]$ and the $[110]$ directions are represented in solid and dotted lines on the right panel respectively. Comparing Fig. 2

with the experimental Fig. 2 in [13], we see that the attenuation peak along $[100]$ coincides almost exactly with the experimental data in the frequency range between 1.38 and 1.70 kHz. In this particular case, the attenuation peaks are also roughly in the same order of magnitude as the observation. Along the $[110]$ direction, the attenuation due to the deaf bands are also nicely recovered by the theory. That is, the two bands predicted by the band structure computation (the second and the third bands in Fig. 2 for the range from M to L) are actually deaf and wave propagation is prohibited within these two bands. Similar results have also been reported for 2D photonic band gap materials [9,19]. Further simulation shows that though the height of the attenuation peaks may vary as the outer boundary of the cylinder arrays changes, the overall shape of the attenuation spectra remain unchanged.

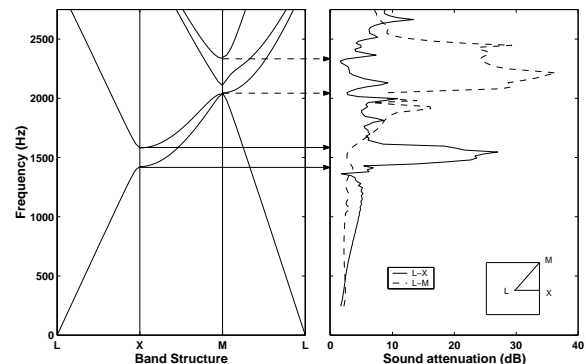


FIG. 2. Right panel: Relative acoustic attenuation vs. frequency for a square array of cylinders with periodicity 11 cm. The radius of the cylinders is 3 cm. Left panel: The band structures computed by the plane wave expansion method.

We also notice that the width of the attenuation peak along $[110]$ is a little wider than the observation. In addition to the aforementioned reasons, this discrepancy could be due to the fact that in the present simulation, the cylinders are assumed to be in the open air, while the experiment was performed in a chamber which may somewhat still reflect sound. Furthermore, the exact number and the setting of the cylinders in the experiment are also not known from the literature. Other contributions to the discrepancy may result from the different acoustic source and receiver used in the theory and experiment. In spite of these limitations, the match between the theory and experiment is quite encouraging.

The band structure shown in Fig. 2 is obtained by using the usual plane-wave method [10]. Here it is shown to agree nicely with the band structure obtained by the variation method calculation. With the parameters in Fig. 2, wave propagation in different directions is inhibited within different frequency regimes. No complete band gap is observed. The overlap of attenuation peaks

along different directions, an indication of the complete band gap, can be observed when cylinder filling factor exceeds certain values [13]; in this case, the matrix inversion in the multiple scattering computation becomes costly.

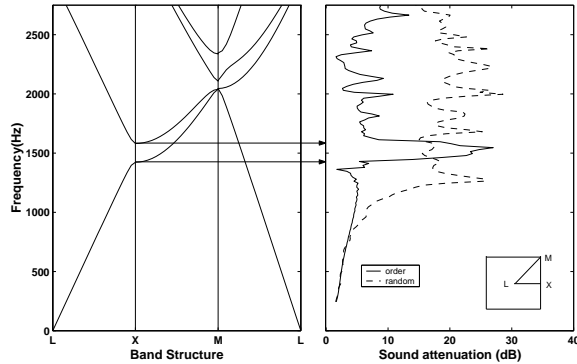


FIG. 3. The right panel shows the relative acoustic attenuation vs. frequency. Here the comparison is made between the results from a square array with periodicity 11 cm (solid line) and from a complete random array of cylinders (dotted line). The radius of the cylinders is 3 cm. Left panel: The band structures computed by the plane wave expansion method.

Now consider the effect of randomness on the acoustic transmission. Here we take the case described by Fig. 2 as the example. While keeping the same cylinder filling and the outer boundary of the array, we allow the cylinders to be distributed completely randomly within the area. The relative attenuation is computed again. The results are shown in Fig. 3, with comparison to the results for wave propagation along [100] for the corresponding square lattice array. The following features are evident. At low frequencies, the introduced disorder does not affect the transmission for the given size of the sample. The randomness reduces the transmission basically for all frequencies above a critical frequency of 700 Hz, except for the frequencies within the lowest stop band along [100] within which though the transmission is still inhibited, the disorder actually reduces the attenuation purely due to the stop-band effect; such a feature is also observed in other acoustic systems [20]. As we increase the sample size, the critical frequency tends to become smaller, implying larger ranges of inhibition. Note that in order to compute the transmission accurately at lower frequencies, larger sample sizes are required and the computation would become costly. The result of the severe reduction in transmission for a wide range of frequencies is remarkable and has significant relevance to the fundamental problem of Anderson localization, a concept originally introduced to explain the conductor-insulator transition induced by disorders in electronic systems [21], because such a reduction is a precursor to the localization phenomenon. The results also imply that random

arrays of rigid cylinders are good candidates in filtering audible noise.

In summary, here we have presented a theory for acoustic transmission through arrays of rigid cylinders in the air. The theory is applied to the experimental situations of regular arrays, yielding favorable agreements. The theoretical results verify the existence of the deaf bands. The results are subsequently extended to the case of random cylinder arrays. We found that wave propagation is significantly reduced by randomness for a wide range of frequencies. This feature makes the rigid cylinders in the air an ideal system for theoretical and experimental studies of wave localization.

The help from E. Hoskinson now at UC Berkeley (Physics) is greatly appreciated. Useful communication with J. Sanchez-Dehesa is also thanked. The work received support from NSC.

-
- [1] A. Ishimaru, *Wave Propagation and Scattering in Random Media*, (Oxford University Press, New York, 1997).
 - [2] Z. Ye, H. Hsu, E. Hoskinson, and A. Alvarez, *Chin. J. Phys.* **37**, 343, (1999).
 - [3] Z. Ye, *J. Appl. Phys.* **78**, 6389 (1995).
 - [4] Z. Ye, T. Curran, and D. Lemon, *ICES J. Mar. Sci.* **53**, 317 (1996).
 - [5] N. M. Lawandy et al. *Nature* **368**, 436 (1994).
 - [6] S. Datta, *Electronic Transport in Mesoscopic Systems*, (Cambridge, N. Y., 1995).
 - [7] C. Kittel, *Introduction to Solid State Physics*, (John Wiley & Son, New York, 1996).
 - [8] e. g. E. Yablonovitch, *Phys. Rev. Lett.* **58**, 2059 (1987); S. John, *Phys. Rev. Lett.* **58**, 2486 (1987).
 - [9] W. Robertson, et al., *Phys. Rev. Lett.* **68**, 2023 (1992).
 - [10] M. S. Kushwaha, *Int. J. Mod. Phys. B* **10**, 977 (1996).
 - [11] R. Martínez-Sala, et al., *Nature* **378**, 241 (1995).
 - [12] M. S. Kushwaha, *Appl. Phys. Lett.* **70**, 3218 (1997).
 - [13] J. V. Sánchez-Pérez, et al., *Phys. Rev. Lett.* **80**, 5325 (1998).
 - [14] E. Hoskinson and Z. Ye, *Phys. Rev. Lett.* **83**, 2734 (1999).
 - [15] V. Twersky, *J. Acoust. Soc. Am.* **24**, 42 (1951).
 - [16] Z. Ye, *Proc. of the National Science Council (ROC)* **A**, *in press*.
 - [17] I. S. Gradshteyn, I. M. Ryzhik, and A. Jeffrey, *Table of Integrals, Series, and Products*, 5th Ed., (Academic Press, New York, 1994).
 - [18] Z. Ye and E. Hoskinson, *Appl. Phys. Lett.* **77**, 4428 (2000).
 - [19] T. F. Krauss, R. M. de la Rue, and S. Brand, *Nature* **383**, 699 (1996).
 - [20] A. R. McGurn, K. T. Christensen, F. M. Mueller, and A. A. Maradudin, *Phys. Rev. B* **47**, 13120 (1993).
 - [21] P. W. Anderson, *Phys. Rev.* **109**, 1492 (1958).